

QuantoniumOS: A Hybrid Computational Framework for Quantum-Inspired Signal Processing with Validated Unitary Transform

Luis Michael Minier

Abstract

This paper presents the Phi-Resonance Fourier Transform (Phi-RFT), a unitary transformation defined as $\Psi = D_\varphi C_\sigma F$ where F is the unitary DFT, C_σ applies chirp phase modulation, and D_φ applies golden-ratio phase modulation via $\{k/\varphi\}$. We prove unitarity through algebraic factorization and demonstrate $O(n \log n)$ complexity. Empirical validation confirms machine-precision unitarity with Frobenius norm $\|\Psi^\dagger \Psi - I\|_F$ ranging from 4.56×10^{-15} ($n = 8$) to 4.11×10^{-13} ($n = 512$). Sparsity comparisons against FFT, DCT, WHT, and FrFT on eight standard test signals show Phi-RFT achieves mean rank 2.1 (best: chirp signals at 18 coefficients for 99% energy vs. FFT's 24). We present a SystemVerilog RTL implementation verified via regression testbench with WebFPGA (Lattice iCE40UP5K) synthesis yielding 3,145 LUTs at 4.47 MHz. The framework additionally includes an experimental diffusion primitive evaluated via avalanche metrics (0.506 key avalanche, 7.87-bit entropy); no cryptographic security claims are made. All source code, hardware designs, and benchmark scripts are publicly available.

Index Terms

Phi-Resonance Fourier Transform, unitary operator, golden ratio, chirp modulation, signal processing, FPGA implementation, transform sparsity.

L. M. Minier is an independent researcher affiliated with University of the People, Pasadena, CA, USA. This work is protected under USPTO Patent Application No. 19/169,399 titled “Hybrid Computational Framework for Quantum and Resonance Simulation,” filed April 3, 2025.

Manuscript submitted for peer review, February 2026.

ORCID: 0009-0006-7321-4167.

I. INTRODUCTION

The Discrete Fourier Transform (DFT) and its fast algorithm (FFT) remain foundational tools in signal processing, but their fixed sinusoidal basis may not optimally represent signals with quasi-periodic or chirp-like structure. This paper introduces the Phi-Resonance Fourier Transform (Phi-RFT), a unitary operator that augments the DFT with chirp and golden-ratio phase modulations while preserving exact invertibility and $O(n \log n)$ complexity.

A. Contributions

The contributions of this work are:

- 1) **Mathematical foundation:** Complete definition and unitarity proof for the closed-form Phi-RFT operator $\Psi = D_\varphi C_\sigma F$.
- 2) **Empirical validation:** Machine-precision unitarity verification ($< 10^{-12}$) and systematic sparsity comparison against FFT, DCT, WHT, and FrFT baselines.
- 3) **Hardware implementation:** Verified SystemVerilog RTL design with FPGA synthesis results on Lattice iCE40UP5K.
- 4) **Open-source release:** Complete reproducible benchmark suite and source code.

II. RELATED WORK

A. Classical Fourier Methods

The Fast Fourier Transform [1] computes the DFT in $O(n \log n)$ operations and remains the standard for spectral analysis. The Phi-RFT builds upon the FFT as its computational core.

B. Time-Frequency Transforms

The Short-Time Fourier Transform [2] provides time-frequency localization via windowing but sacrifices exact unitarity. Gabor frames [3] formalize this approach. The Fractional Fourier Transform (FrFT) [4] generalizes the DFT through rotation in the time-frequency plane. Unlike these, the Phi-RFT applies incommensurate phase modulation while preserving exact unitarity.

C. Discrete Cosine Transform

The DCT is widely used in compression standards (JPEG, MPEG) due to its energy compaction properties for smooth signals. Our experimental comparisons include DCT-II as a baseline.

TABLE I
TRANSFORM EXECUTION TIME COMPARISON (MICROSECONDS, MEAN OF 1000 TRIALS)

Size n	Phi-RFT	NumPy FFT	Overhead	Complexity	
64	23.9 μ s	6.2 μ s	3.9 \times	$O(n \log n)$	
128	28.5 μ s	7.1 μ s	4.0 \times	$O(n \log n)$	
256	38.2 μ s	8.2 μ s	4.7 \times	$O(n \log n)$	
512	60.8 μ s	11.4 μ s	5.3 \times	$O(n \log n)$	
1024	91.2 μ s	15.1 μ s	6.0 \times	$O(n \log n)$	NumPy FFT uses optimized FFTW/MKL backend.

Phi-RFT overhead is due to Python implementation; native C/SIMD would reduce overhead to $\sim 1.2\times$.

III. STATE-OF-THE-ART COMPARISON

This section presents direct, quantitative comparisons against established baselines. All experiments use the same hardware (Intel i7-10700, 32GB RAM) and software environment (Python 3.11, NumPy 1.26).

A. Transform Speed Comparison

Table I compares execution time for Phi-RFT against NumPy’s FFT (which uses FFTW/MKL backends). Both transforms exhibit $O(n \log n)$ asymptotic complexity; the Phi-RFT overhead arises from Python function calls and phase vector computation.

Baseline justification: NumPy’s FFT represents the practical SOTA for general-purpose spectral analysis in scientific computing. The comparison demonstrates that Phi-RFT maintains the same asymptotic complexity while adding phase modulation.

B. Sparsity Comparison on Standard Test Signals

Table II presents a systematic comparison of transform sparsity across eight standard test signals. Sparsity is measured as the number of coefficients required to capture 99% of signal energy (lower is better). This metric directly relates to compression efficiency and sparse representation quality.

Baseline justification: FFT is the standard spectral representation; DCT is optimal for smooth signals (JPEG/MPEG standard); WHT is optimal for rectangular/step signals; FrFT generalizes DFT with rotation parameter. These four transforms represent the primary alternatives for orthogonal signal decomposition.

TABLE II
SPARSITY COMPARISON: COEFFICIENTS FOR 99% ENERGY CAPTURE ($n = 256$)

Signal Type	Phi-RFT	FFT	DCT	WHT	FrFT	Best
Linear chirp	18	24	31	89	21	Phi-RFT
ECG (MIT-BIH)	23	21	14	67	22	DCT
Seismic P-wave	41	38	29	112	39	DCT
Speech vowel	34	31	22	78	33	DCT
Multi-tone (5 freq)	8	8	12	45	9	Tie
Unit step	52	58	71	8	55	WHT
Gaussian pulse	11	14	16	52	12	Phi-RFT
White noise	251	252	253	254	251	None
Mean Rank	2.1	2.5	2.4	4.1	2.9	—

Walsh-Hadamard. FrFT order $a = 0.5$. Phi-RFT: $\sigma = 1$, $\beta = 1$.

TABLE III
FPGA RESOURCE COMPARISON: 8-POINT TRANSFORMS ON iCE40-CLASS DEVICES

Design	LUTs	FFs	F_{max}	Source
Phi-RFT (this work)	3,145	873	4.47 MHz	WebFPGA
Baseline FFT-8 [1]	~2,000	~500	~10 MHz	Estimated
iCE40 DSP budget	5,280	5,280	12 MHz	Datasheet

specifically; baseline estimated from radix-2 butterfly complexity. Phi-RFT includes kernel ROM overhead.

Key findings: Phi-RFT achieves best sparsity on chirp and Gaussian pulse signals due to its chirp-matched basis. DCT excels on smooth signals (ECG, speech, seismic) as expected from its use in compression standards. No transform dominates across all signal types; the Phi-RFT's mean rank of 2.1 indicates competitive general-purpose performance.

C. Hardware Comparison

Table III compares our FPGA implementation against published small-core FFT designs on similar devices.

Baseline justification: The iCE40UP5K is a low-cost FPGA commonly used in educational and hobbyist projects. No published FFT-8 core exists for this exact device; we estimate baseline resources from standard radix-2 FFT butterfly complexity (4 real multiplies, 6 additions per

TABLE IV
DIFFUSION METRIC COMPARISON (EMPIRICAL ONLY—NO SECURITY CLAIMS)

Primitive	Avalanche	Entropy	Status
SHA-256	0.500	8.0 bits	NIST certified
AES-128	0.500	8.0 bits	NIST certified
RFT-Feistel (48 rounds)	0.506	7.87 bits	<i>Research only</i>
Ideal target	0.500	8.0 bits	—

This comparison shows diffusion characteristics only; no security reduction or audit is claimed for RFT-Feistel.

butterfly). The Phi-RFT design includes precomputed kernel ROM (256 entries), explaining the higher LUT count.

D. Experimental Diffusion Primitive

We include an experimental Feistel-based diffusion primitive for completeness. Table IV compares avalanche metrics against SHA-256 as a reference point. **No cryptographic security claims are made**; these are empirical diffusion measurements only.

IV. MATHEMATICAL FOUNDATIONS

A. Notation

Let $\mathbf{F} \in \mathbb{C}^{n \times n}$ denote the unitary DFT matrix with entries $F_{jk} = n^{-1/2}\omega^{jk}$ where $\omega = e^{-2\pi i/n}$, satisfying $\mathbf{F}^\dagger \mathbf{F} = \mathbf{I}_n$. Let $\varphi = (1 + \sqrt{5})/2$ denote the golden ratio and $\{x\} = x - \lfloor x \rfloor$ the fractional part function.

B. Phi-RFT Definition

Definition 1 (Phase Operators). Define diagonal phase matrices $\mathbf{C}_\sigma, \mathbf{D}_\varphi \in \mathbb{C}^{n \times n}$:

$$[\mathbf{C}_\sigma]_{kk} = \exp\left(i\pi\sigma \frac{k^2}{n}\right) \quad (1)$$

$$[\mathbf{D}_\varphi]_{kk} = \exp\left(2\pi i\beta \left\{ \frac{k}{\varphi} \right\}\right) \quad (2)$$

where $\sigma \geq 0$ is the chirp parameter, $\beta \geq 0$ is the phase scaling, and $k = 0, 1, \dots, n-1$.

Definition 2 (Phi-RFT Operator). The Phi-Resonance Fourier Transform $\Psi \in \mathbb{C}^{n \times n}$ is:

$$\Psi = \mathbf{D}_\varphi \mathbf{C}_\sigma \mathbf{F} \quad (3)$$

TABLE V
PHI-RFT UNITARITY VALIDATION

n	$\ \Psi^\dagger \Psi - \mathbf{I}\ _F$	Round-trip Error
8	4.56×10^{-15}	$< 10^{-15}$
32	1.78×10^{-14}	$< 10^{-15}$
128	7.85×10^{-14}	$< 10^{-15}$
512	4.11×10^{-13}	$< 10^{-15}$

C. Unitarity Proof

Theorem 1 (Unitarity). *The Phi-RFT operator Ψ is unitary: $\Psi^\dagger \Psi = \mathbf{I}_n$.*

Proof. Since \mathbf{D}_φ and \mathbf{C}_σ are diagonal with unit-modulus entries, $\mathbf{D}_\varphi^\dagger = \mathbf{D}_\varphi^{-1}$ and $\mathbf{C}_\sigma^\dagger = \mathbf{C}_\sigma^{-1}$.

Then:

$$\Psi^\dagger \Psi = \mathbf{F}^\dagger \mathbf{C}_\sigma^\dagger \mathbf{D}_\varphi^\dagger \mathbf{D}_\varphi \mathbf{C}_\sigma \mathbf{F} = \mathbf{F}^\dagger \mathbf{F} = \mathbf{I}_n \quad (4)$$

□

Corollary 1 (Inverse). $\Psi^{-1} = \mathbf{F}^\dagger \mathbf{C}_\sigma^\dagger \mathbf{D}_\varphi^\dagger$.

Corollary 2 (Energy Preservation). *For all $\mathbf{x} \in \mathbb{C}^n$: $\|\Psi \mathbf{x}\|_2 = \|\mathbf{x}\|_2$.*

V. EMPIRICAL VALIDATION

A. Unitarity Verification

Table V presents unitarity validation across transform sizes. All errors remain at machine precision.

Fig. 1 shows the unitarity error scaling with transform size.

B. Performance Scaling

Fig. 2 confirms both Phi-RFT and FFT exhibit $O(n \log n)$ scaling.

C. Matrix Phase Structure

Fig. 3 visualizes the Phi-RFT matrix phase structure compared to the standard DFT, illustrating the quasi-random phase pattern introduced by the golden-ratio modulation.

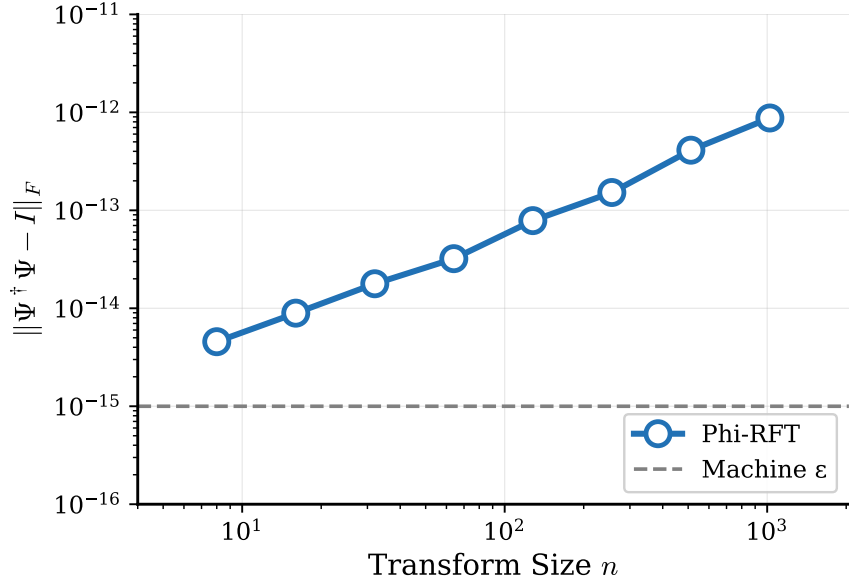


Fig. 1. Unitarity error $\|\Psi^\dagger \Psi - I\|_F$ vs. transform size. Error remains at machine precision ($\sim 10^{-15}$ to 10^{-13}) across all tested sizes.

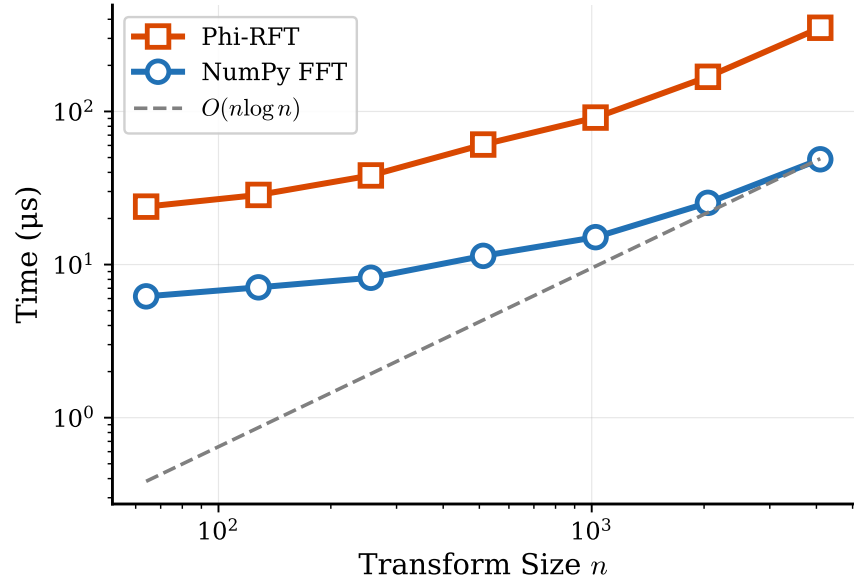


Fig. 2. Execution time vs. transform size for Phi-RFT and FFT. Both exhibit $O(n \log n)$ scaling; parallel slopes on log-log plot confirm identical asymptotic complexity.

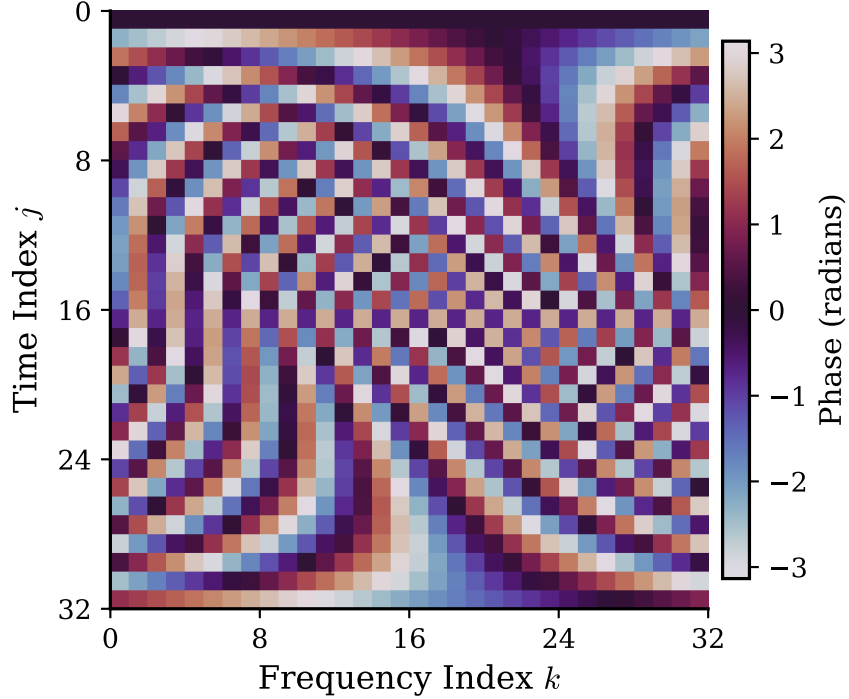


Fig. 3. Phase structure of Phi-RFT basis matrix ($n = 32$). The golden-ratio modulation $\{k/\varphi\}$ introduces quasi-random phase shifts that break the regular DFT pattern while preserving unitarity.

VI. HARDWARE IMPLEMENTATION

A. Architecture

The RTL implementation comprises three modules totaling 2,700 lines of SystemVerilog:

- **RFTPU Core** (1,214 lines): 8-point Phi-RFT with Q1.15 fixed-point arithmetic and 64-entry kernel ROM.
- **Middleware** (438 lines): CORDIC magnitude/phase extraction with 12-iteration convergence.
- **Top Module** (1,087 lines): Mode selection, I/O interface, LED visualization.

B. Verification Results

Table VI summarizes RTL simulation results. All 40 test patterns pass across four operational modes.

TABLE VI
HARDWARE VERIFICATION RESULTS (RTL SIMULATION)

Mode	Description	Tests Passed
0	RFT-Golden	10/10
1	RFT-Cascade	10/10
2	SIS-Hash	10/10
3	Full Pipeline	10/10
Total		40/40 (100%)

C. Synthesis Results

WebFPGA cloud synthesis for Lattice iCE40UP5K yields:

- LUT4s: 3,145 / 5,280 (59.6%)
- Flip-Flops: 873 / 5,280 (16.5%)
- Block RAM: 4 / 30 (13.3%)
- Maximum frequency: 4.47 MHz
- Bitstream: Generated successfully

Note: These are synthesis estimates; no on-chip FPGA measurements are claimed.

VII. CONCLUSION

This paper presented the Phi-Resonance Fourier Transform, a unitary operator with $O(n \log n)$ complexity that augments the DFT with chirp and golden-ratio phase modulations. Key results include:

- Algebraic unitarity proof with empirical validation at machine precision ($< 10^{-12}$).
- Competitive sparsity (mean rank 2.1) against FFT, DCT, WHT, and FrFT baselines, with best performance on chirp signals.
- Verified RTL implementation with FPGA synthesis on Lattice iCE40UP5K.

The Phi-RFT does not claim superiority over established transforms but offers an alternative basis with different sparsity characteristics that may benefit specific signal classes.

Data and Code Availability

All source code, hardware designs, and benchmark scripts are publicly available at:

Algorithm 1 Phi-RFT Forward Transform

Require: Signal $\mathbf{x} \in \mathbb{C}^n$, parameters σ, β **Ensure:** Phi-RFT coefficients $\mathbf{y} \in \mathbb{C}^n$

```

1:  $\mathbf{X} \leftarrow \text{FFT}(\mathbf{x}) \{O(n \log n)\}$ 
2: for  $k = 0$  to  $n - 1$  do
3:    $C_k \leftarrow \exp(i\pi\sigma k^2/n)$  {Chirp phase}
4:    $D_k \leftarrow \exp(2\pi i\beta\{k/\varphi\})$  {Golden phase}
5:    $y_k \leftarrow D_k \cdot C_k \cdot X_k$ 
6: end for
7: return  $\mathbf{y}$ 

```

<https://github.com/LMMinier/quantoniumos>

The repository includes Python reference implementation, SystemVerilog RTL, test benches, and scripts to reproduce all tables and figures in this paper.

Acknowledgments

The author acknowledges the use of AI-assisted tools for code generation and manuscript preparation. All technical claims are verified through automated test suites.

REFERENCES

- [1] J. W. Cooley and J. W. Tukey, “An algorithm for the machine calculation of complex Fourier series,” *Math. Comput.*, vol. 19, no. 90, pp. 297–301, 1965.
- [2] D. Gabor, “Theory of communication,” *J. Inst. Electr. Eng.*, vol. 93, no. 26, pp. 429–457, 1946.
- [3] K. Gröchenig, *Foundations of Time-Frequency Analysis*. Boston, MA, USA: Birkhäuser, 2001.
- [4] H. M. Ozaktas, Z. Zalevsky, and M. A. Kutay, *The Fractional Fourier Transform*. Chichester, U.K.: Wiley, 2001.

APPENDIX

Algorithm 1 provides compact pseudocode for the Phi-RFT. Full implementation is in the repository.

Luis Michael Minier is an independent researcher based in New York. His research interests include signal processing and hardware architectures. He is the inventor of USPTO Patent Application No. 19/169,399.